Oscillations of critical superconducting current in thin doubly-connected Sn films in an external perpendicular magnetic field

A. G. Sivakov,[a] A. S. Pokhila, A. M. Glukhov, S. V. Kuplevakhsky, and A. N. Omelyanchouk

B. Verkin Institute for Low Temperature Physics and Engineering of the National Academy of Sciences of Ukraine, 47 Lenin Ave., Kharkov 61103, Ukraine

(Submitted September 5, 2013)
Fiz. Nizk. Temp. **40**, 527–538 (May 2014)

We report the results of experimental and theoretical studies of critical current oscillations in thin doubly-connected Sn films in an external perpendicular magnetic field. The experiments were performed on samples that consisted of two wide electrodes joined together by two narrow channels. The length of the channels l satisfied the condition $l \gg \xi$ (ξ is the Ginzburg–Landau coherence length). At temperatures close to the critical temperature T_c, the dependence of the critical current I_c on average external magnetic flux $\bar{\Phi}_e$ has the form of a piecewise linear function, periodic with respect to the flux quantum Φ_0. The amplitude of the I_c oscillation at a given temperature is proportional to the factor ξ/l. Moreover, the dependence $I_c = I_c(\bar{\Phi}_e)$ is found to be multivalued, hence indicating the presence of metastable states. Based on the Ginzburg–Landau approximation, a theory was constructed that explains the above features of the oscillation phenomenon taking a perfectly symmetric system as an example. Further, the experiments displayed the effects related to the critical currents imbalance between the superconducting channels, i.e., shift of the maxima of the dependence $I_c = I_c(\bar{\Phi}_e)$ accompanied by an asymmetry with respect to the transport current direction. © *2014 AIP Publishing LLC*. [http://dx.doi.org/10.1063/1.4876229]

1. Introduction

Off-diagonal long-range order,[1,2] which is responsible for the phenomenon of superconductivity, manifests itself in the form of various oscillation effects in doubly-connected superconducting systems in external magnetic fields. Such effects include, for instance, the Little-Parks resistance oscillations in superconducting thin-walled cylinders and narrow rings,[3–8] as well as the oscillations of the critical transport current I_c in superconducting interferometers consisting of a loop with two parallel Josephson junctions.[9–11] The oscillations of both types are periodic in the flux of an external magnetic field with a period equal to one flux quantum $\Phi_0 = \pi\hbar c/|e|$.

Recently, the possibility of creating superconducting interferometers containing no artificial Josephson junctions attracted significant interest of experimentalists (see Refs. 12–15). Such a possibility has long been discussed in theoretical studies,[16] where, within the framework of Ginzburg-Landau theory,[17] a simple doubly-connected superconducting circuit has been considered. The circuit was formed by uniform and effectively one-dimensional elements: a circular loop of a small radius and two long linear electrodes.

Critical current oscillations has been predicted in Ref. 16 and observed for the first time in Ref. 13. In the experiments reported in Ref. 14, the superconducting devices similar to the interferometers proposed in Ref. 16 have been studied. However, the role of loops in the experiments was played by composite rings consisting of two halves with different critical currents. As expected (see, e.g., Refs. 18 and 19), the dependences of $I_c = I_c(\Phi_e/\Phi_0)$ obtained by Gurtovoĭ *et al.*[14] showed characteristic shifts of the critical current maxima with respect to the points $\Phi_e/\Phi_0 = 0, \pm 1, \pm 2, \ldots$ as well as an asymmetry with respect to the transport current direction.

In accordance with the theory,[16] Refs. 13 and 14 employed "microscopic" doubly-linked elements (superconducting loops and rings) with the linear dimensions not exceeding the temperature-dependent coherence length $\xi(T)$.[4–6] To ensure that this condition is fulfilled, aluminum, which is characterized by a large BCS coherence length ξ_0,[20] was selected as the superconducting material, and the measurements were carried out at temperatures close to the critical temperature T_c.

However, the experiments[12] on wide tin films with a macroscopic rectangular hole convincingly demonstrated that "microscopicity" of a doubly-connected superconducting system is not a prerequisite for the observation of critical current oscillations. The same conclusion was also drawn by Michotte *et al.*,[15] who have studied experimentally the oscillatory dependence of $I_c = I_c(\Phi_e/\Phi_0)$ for niobium loops with symmetric and asymmetric injection of transport current. A distinctive feature of the experiments in Ref. 15 was the fact that the measurements were performed at low temperatures as compared to T_c, when the "microscopicity" condition is clearly not fulfilled.

In a series of our experiments we observed oscillations of the critical transport current in a doubly-connected macroscopic superconducting system at temperatures close to T_c. In this paper, we present the main results of these experiments, as well as their consistent theoretical interpretation within the framework of the Ginzburg-Landau approximation.

The samples for our experiments were prepared using tin thin films and shaped as two long narrow ($l \gg \xi(T)$) channels connected to wide electrodes (see Fig. 1). The following basic properties of macroscopic oscillation effect were experimentally established: the dependence $I_c = I_c(H_e)$ (H_e is the external magnetic field) exhibits a piecewise linear behavior and is multivalued, while the oscillation amplitude is proportional to the factor $\xi(T)/l$. These properties were fully explained by the developed theory.

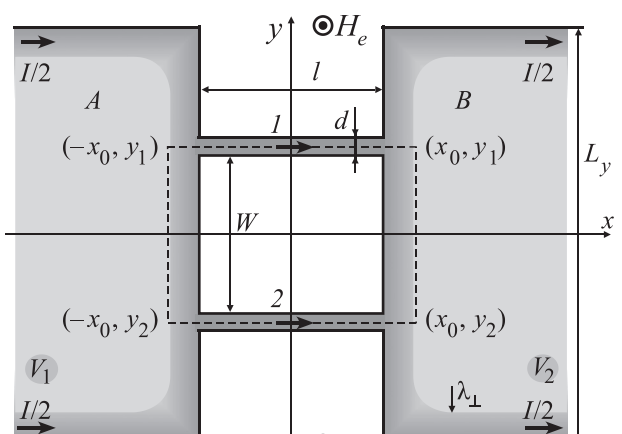

FIG. 1. Schematic experimental geometry in the plane $z = 0$. The regions where perpendicular magnetic field penetrates into the sample are shaded. Gray circles indicate the locations of potential contacts V_1 and V_2. (See the text, Sec. 2 and 3, for further details.)

We also observed the effects of asymmetry, which have been found in earlier studies.[14,15] In this paper, such effects are qualitatively explained by the fact that the long superconducting channels were not fully identical.

Sec. 2 describes the experimental setup and basic experimental results. In Sec. 3, a theory of macroscopic oscillation effect in the case of a perfectly symmetric system is developed. Finally, in Sec. 4, we formulate the main results of the study and give some concluding remarks.

2. Experimental methods and main experimental results

Fig. 1 schematically illustrates the geometry of the experiment. Superconducting sample is shown in gray. It is a doubly-connected thin-film structure which consists of two wide electrodes A and B, joined by two narrow channels 1 and 2. External magnetic field $\mathbf{H}_e$ is directed along the z-axis ($\mathbf{H}_e = (0,0,H_e)$), and the transport current $\mathbf{I}$ is injected along the x-axis ($\mathbf{I} = (I,0,0)$).

The experiments were conducted using a set of samples that had the same shape, but a different length l of the superconducting channels. Samples were prepared by electron-beam lithography; tin, which is a type-I superconductor, was used as the film material.[4]

The basic geometrical parameters of the samples were as follows: the film thickness $t = 0.25$ μm, the channel width $d = 0.3$ μm, and the distance between the channels $w = 5$ μm. The length l of the channels varied from 5 to 110 μm.

The critical temperature T_c, measured as the end of the superconducting transition, was from 3.825 to 3.915 K for different samples. The experiments were performed in the temperature range $\Delta T = 0.90$–$0.99T_c$. Temperature was maintained with an accuracy equal or better than $0.0005(T/T_c)$. Earth's magnetic field was shielded using a three-layer permalloy (over 100-fold attenuation) and a superconducting shields.

All samples were of sufficiently high purity: the estimated mean free path was 0.117 μm. (Note that for tin $\xi_0 = 0.23$ μm and the depth of penetration in the clean limit at zero temperature $\lambda(0) \approx 0.05$ μm.[4]) In the entire temperature range of the measurements ΔT, the condition of smallness for the transverse dimensions t and d of the channels with respect to the temperature-dependent coherence length $\xi(T)$ ($\xi(T) \propto \xi_0(1 - T/T_c)^{-1/2}$) was satisfied. However, the temperature-dependent penetration depth $\lambda(T) \propto \lambda(0)(1 - T/T_c)^{-1/2}$ was of the order of or smaller than t and d.

In the experiments, current-voltage characteristics (CVC) were measured as a function of the applied magnetic field H_e. The current-voltage characteristics of all samples exhibited a shape typical for the resistivity mechanism associated with the formation of phase slip centers[5,6,21] (see Fig. 2).

Once the critical current was reached, the voltage appeared abruptly, and switching to the steps with linear and differential resistance, which was a multiple of a certain value, and the same excess current was observed. Thus, the value of critical current was well fixed and not dependent on the voltage level at which the critical current was measured in the switching region. In this case, the critical current at which a jump to the first step occurred varied periodically with magnetic field between the values $I_{c\ max}$ and $I_{c\ min}$. The currents at which the jumps to the second and all subsequent steps occurred did not oscillate with magnetic field. Neither the excess current nor the differential resistance of the steps exhibited magnetic field dependence and, therefore, the voltage drop at the steps did not oscillate either at a fixed current.

Based on the conducted experiments, two types of behaviour were established. The first type (I) is characterized by the basic properties of the macroscopic oscillation effect, while the patterns of the second type (II) presumably appeared due to the incomplete symmetry of the samples.

Basic properties of macroscopic oscillation effect (type I)

All the obtained dependences $I_c = I_c(H_e)$ exhibited pronounced periodicity, oscillatory behavior, and piecewise-linear shape (see Figs. 3, 5, 7, and 8). The oscillation period ΔH_e did not depend on temperature.

The quotient of division of the magnetic flux quantum Φ_0 by the oscillation period for each of the samples was equal to the area bounded by a certain effective loop (see Fig. 1) which

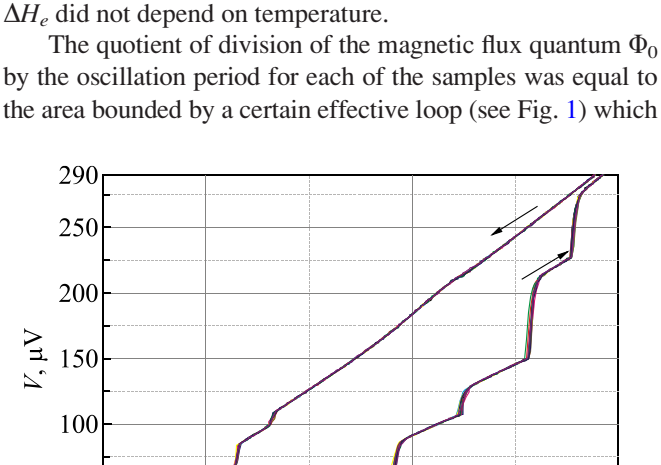

FIG. 2. Set of current-voltage characteristics of the sample with the channel length $l = 25$ μm measured at the reduced temperature $T/T_c = 0.976$ in different magnetic fields.

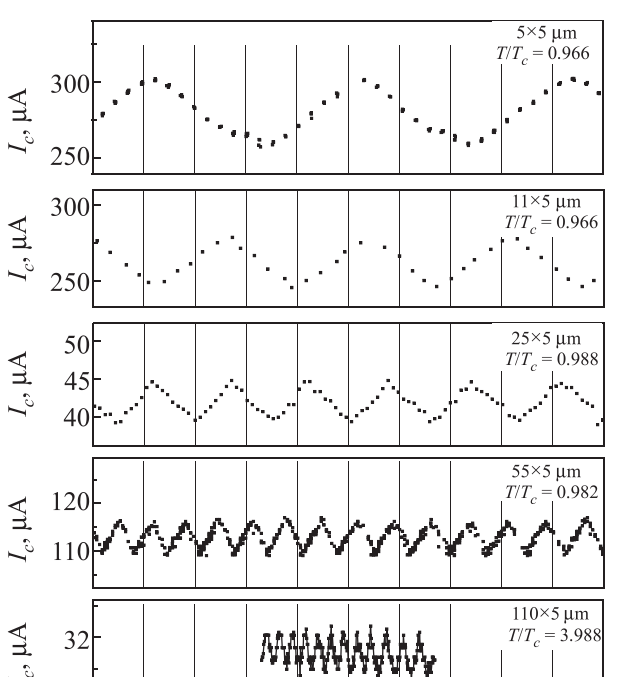

FIG. 3. $I_c(H_e)$ plots for the samples with different channel lengths (l = 5, 11, 25, 55, 110 μm). The oscillation period ΔH_e is approximately inversely proportional to the area of the opening.

was entirely located within the film and surrounding the hole. The area bounded by the effective contour was always slightly larger than the orifice area and was approaching it upon increasing the length of the channel l (see Fig. 3 for illustration).

Using the samples with different channel lengths in the experiments allowed us to establish the fact of linear dependence of the oscillation amplitude $I_c = I_c(H_e)$ on $1/l$ at a given temperature (see Fig. 4).

The critical current $\bar{I}_c$ averaged over the oscillation period increased with decreasing temperature as $\bar{I}_c \propto (1 - T/T_c)^{3/2}$. The oscillation amplitude ΔI_c initially increased and then, at a reduced temperature $T/T_c < 0.9$, tended to saturate.

Moreover, upon decreasing temperature, when a hysteresis appeared in CVC, the dependences $I_c = I_c(H_e)$ became multivalued (Figs. 5, 7, and 8). This was revealed

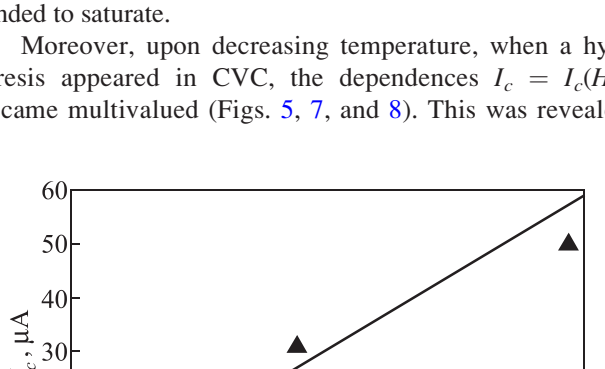

FIG. 4. Dependence of the oscillation amplitude ΔI_c on the channel length l at the reduced temperature $T/T_c = 0.97$.

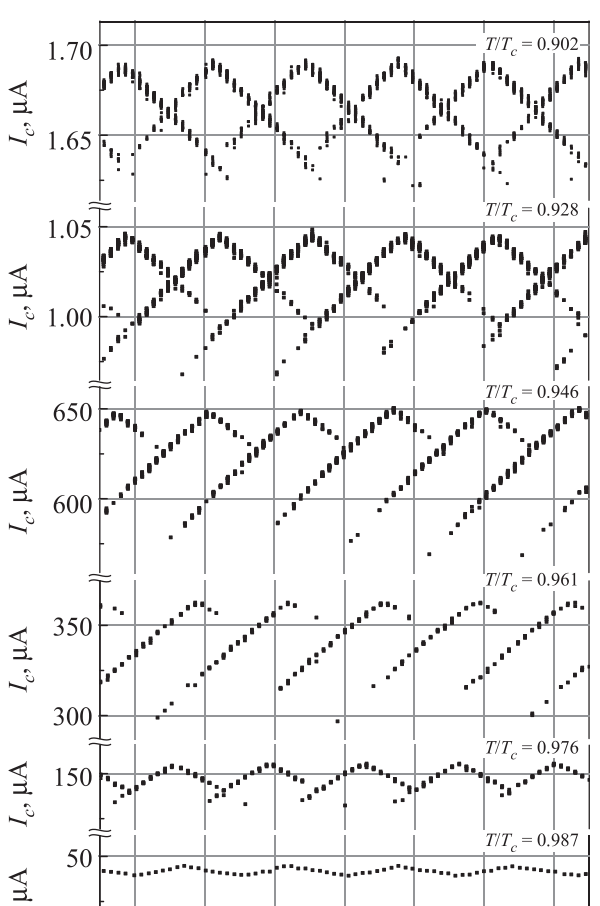

FIG. 5. Magnetic field dependence of the critical field for the sample with l = 25 μm at different temperatures. The values of critical current were determined from the current-voltage characteristics measured several times at the same value of magnetic fields.

by recording CVCs multiple times at a fixed value of a magnetic field (Fig. 6). Thus, the longer the sample was, the more branches $I_c = I_c(H_e)$ were observed (cf. Fig. 7 (l = 5 μm), 5 (l = 25 μm), and 8 (l = 55 μm)).

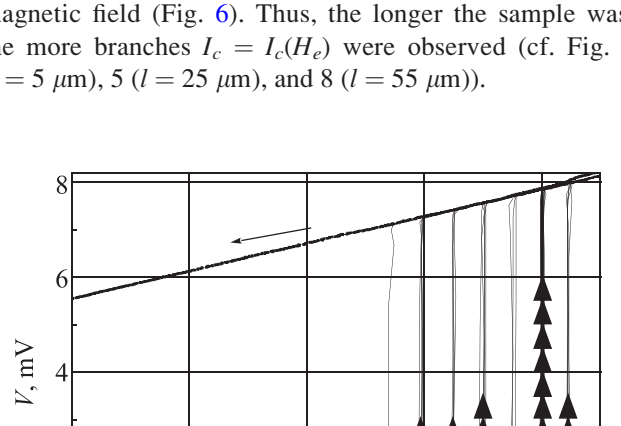

FIG. 6. Current-voltage characteristic of the sample with the channel length l = 55 μm ($T/T_c = 0.911$, H = 0.6 Oe) obtained at a fixed value of the magnetic field measured at the reduced temperature $T/Tc = 0.976$ in different magnetic fields.

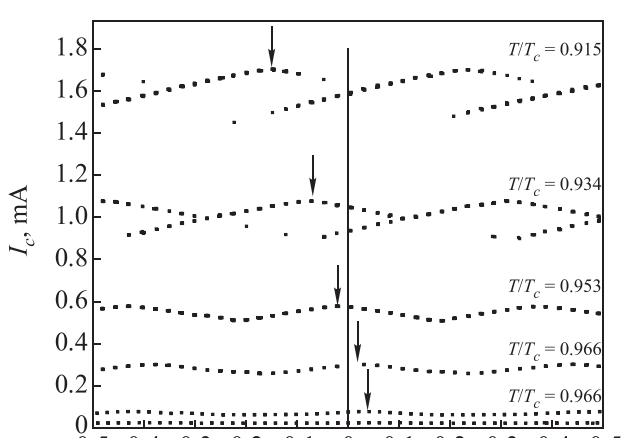

FIG. 7. Temperature shift of the critical current maximum in the dependence $I_c = I_c(H_e)$ for the sample with the channel length $l = 5$ μm.

Asymmetry effects (type II)

Almost for all the samples (Figs. 3, 5, 7, and 8), the dependence $I_c = I_c(H_e)$ exhibited an offset of the critical current maximum point from $H_e = 0$. The offset varied when the temperature was changed (see Fig. 7).

The offset of the critical current maximum was accompanied by an asymmetry of the dependence $I_c = I_c(H_e)$ with respect to reversal of the transport current direction. This asymmetry increased with decreasing temperature, and, ultimately, the plots $I_c = I_c(H_e)$ acquired a sawtooth-like shape (see Fig. 8), which indicated a transition to the resistive state of only one of the two superconducting channels.

Note that the above described phenomena have also been observed in the experiments of Refs. 14 and 15 on specially prepared asymmetric samples. Moreover, such effects have long been studied and discussed in detail for the case of superconducting interferometers containing two Josephson junctions with different critical currents.[18,19] Following the arguments of Refs. 18 and 19, we can conclude that in our case the asymmetry effects arise due to unequal critical currents of the two superconducting channels, which, apparently, results from the inevitable presence of microstructural defects.

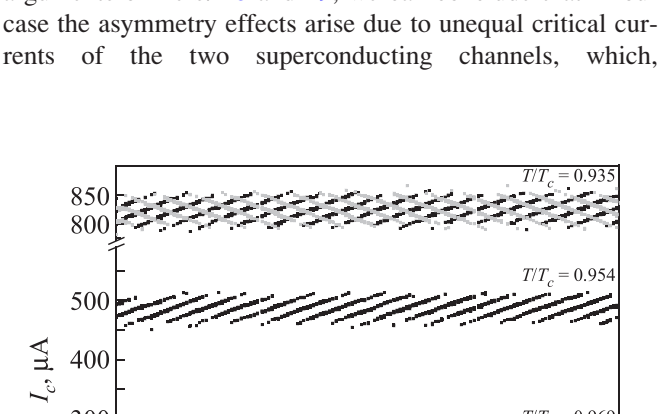

FIG. 8. $I_c = I_c(H_e)$ dependences for the sample with $l = 55$ μm measured at different temperatures and fixed (positive) direction of the transport current (three lower graphs). With decreasing temperature the dependences become sawtooth-like. The upper graph ($T/T_c = 0.935$) shows the dependence $I_c = I_c(H_e)$ for the two directions of the transport current.

3. Theory of the oscillatory effect in the case of a fully symmetric system

For a theoretical explanation of the main experimentally observed features of the macroscopic oscillation effect (Sec. 2, type-I behavior) it is sufficient to consider the simplest case of a fully symmetric system. In particular, in this section we will assume that the experimental model shown in Fig. 1 is fully symmetric with respect to reflections in the planes $x = 0$, $y = 0$, and $z = 0$, implying that the critical currents of superconducting channels *1* and *2* are identical.

Since the condition

$$1 - T/T_c \ll 1\,, \tag{1}$$

was satisfied in all the measurements (temperature range $\Delta T = 0.90$–$0.99T_c$), the local Ginzburg-Landau equations will serve as a departure point for our theory.[17] However, first we need to make an important remark.

As follows from the microscopic theory (see, e.g., Ref. 4), to fulfill the local approximation, in addition to the condition (1), two more conditions are required. First, the smallest linear dimensions of the system (the film thickness t and channel width d) should satisfy the inequality

$$\xi_0 < t, d\,, \tag{2}$$

where ξ_0 is the BCS coherence length.[20] Second, the inequality providing the local coupling between the superconducting current $\mathbf{j}$ and the vector potential $\mathbf{A}$ should be fulfilled as well:

$$\xi_0 < \lambda\,, \tag{3}$$

where $\lambda = \lambda(T)$ is the Ginzburg-Landau penetration depth. While inequality (2) can be assumed to hold always, the inequality (3) will be satisfied for some samples only at the upper limit of the temperature interval ΔT. Fortunately, this does not affect the explanation of the oscillation effect and will be ignored hereafter.

So, once again let us consider the geometry of the problem (Fig. 1). We denote the spatial region occupied by the sample as Ω (colored gray in Fig. 1). Since the sample is made of a type-I superconductor, the following condition is satisfied

$$\lambda \ll \xi\,, \tag{4}$$

where $\xi = \xi(T)$ is the Ginzburg-Landau coherence length.

The superconducting electrodes A and B will be considered semi-infinite in the x-direction (i.e., $L_x \to \infty$). The other linear dimensions of the system satisfy the following conditions, which are fulfilled in the experiment:

$$t, d \ll \xi\,, \tag{5}$$

$$t, d \sim \lambda\,, \tag{6}$$

$$w \gg t, d\,, \tag{7}$$

$$l/2 \gg \xi\,, \tag{8}$$

$$(L_y - w)/2 \gg \lambda_\perp , \tag{9}$$

where $\lambda_\perp$ is the penetration depth for a perpendicular magnetic field,[4,5,22] for which, in our case, the following estimate is valid

$$t, d, \lambda < \lambda_\perp < \xi . \tag{10}$$

The role of conditions (5)–(10) will be clarified in what follows.

The superconducting state is described by the Ginzburg-Landau equation for the complex order parameter $\Delta = \Delta(\mathbf{r})$, which is continuous and single-valued[23] in the whole region Ω and can be represented in the following form:

$$\Delta = \Delta_0 f \, \mathrm{e}^{-i\chi} . \tag{11}$$

Here, $\Delta_0 = \Delta_0(T)$ is the real order parameter for an unperturbed bulk superconductor and the real function $f = f(\mathbf{r})$ (the reduced modulus of the order parameter) takes values within the interval (0,1] and satisfies the boundary condition:

$$(\nabla f \cdot \mathbf{n})|_{\mathbf{r}\in\partial\Omega} = 0 , \tag{12}$$

where $\mathbf{n} = (n_x, n_y, n_z)$ is the outward normal to the surface $\partial\Omega$. From the condition of uniqueness of the order parameter, the boundary condition for the phase χ is

$$\oint_\Gamma (\nabla\chi \, d\mathbf{r}) = 2\pi N \quad (N = 0, \pm 1, \pm 2, \ldots), \tag{13}$$

where Γ is an arbitrary continuous closed contour enclosing the opening in the system. (One such circuit within the plane $z = 0$ is shown in Fig. 1.) Recall that a topological number N, appearing in the right-hand side of Eq. (13), parameterizes different allowed states of the system for a given value of an external field H_e (see, e.g., Ref. 24).

The complete system of equations also includes the Maxwell equations

$$\mathrm{rot}\,\mathbf{h} = \frac{4\pi}{c}\mathbf{j}, \quad \mathbf{h} = \mathrm{rot}\,\mathbf{A} , \tag{14}$$

where $\mathbf{h} = (h_x, h_y, h_z)$ is the local magnetic field, which satisfies the boundary conditions:

$$\mathbf{h}|_{y=\pm\infty} = \mathbf{h}|_{z=\pm\infty} = (0, 0, H_e) , \tag{15}$$

and $\mathbf{A} = (A_x, A_y, A_z)$ is the corresponding vector potential. The superconducting current density $\mathbf{j}$ satisfies the continuity condition

$$\mathrm{div}\,\mathbf{j} = 0 \tag{16}$$

and the boundary condition

$$(\mathbf{j} \cdot \mathbf{n})|_{\mathbf{r}\in\partial\Omega} = 0. \tag{17}$$

It is given by the Ginzburg-Landau relation

$$\mathbf{j} = \frac{c\Phi_0}{8\pi^2\lambda^2} f^2 \left(\nabla\chi - \frac{2\pi\mathbf{A}}{\Phi_0} \right), \tag{18}$$

where $\Phi_0 = \pi\hbar c/|e|$ is the magnetic flux quantum. Note that due to Eq. (17) and the symmetry of the problem, $j_z \equiv 0$. Therefore, it is logical to use the gauge

$$A_z \equiv 0, \tag{19}$$

at which

$$\chi = \chi(x, y). \tag{20}$$

For convenience, we label the quantities Δ and $\mathbf{j}$ in the region of electrodes with the indices A and B and those in the region of channels with the indices 1 and 2:

$$\begin{aligned} &\Delta_{A,B} = \Delta_0 f_{A,B} \mathrm{e}^{-i\chi}, \;\; \Delta_{1,2} = \Delta_0 f_{1,2} \, \mathrm{e}^{-i\chi}; \\ &\mathbf{j}_{A,B} = (j_{Ax,Bx}, j_{Ay,By}, 0), \;\; \mathbf{j}_{1,2} = (j_{1,2}, 0, 0). \end{aligned} \tag{21}$$

Due to the boundary condition (12) and strong inequalities (5),[2,4,8]

$$f_{A,B} = f_{A,B}(x, y), \; f_{1,2} = f_{1,2}(x). \tag{22}$$

(Note that, due to relations (20) and (22), the whole dependence of the current densities $\mathbf{j}_{A,_B}$ and $\mathbf{j}_{1,2}$ on the z-coordinate is transferred to the components of the vector potential $\mathbf{A}$; see definition (18).)

At the boundaries between the electrodes and channels the conditions of continuity are fulfilled:

$$\begin{aligned}
&f_1\left(-\frac{l}{2}\right) = \frac{1}{d}\int_{-w/2-d}^{-w/2} dy f_A\left(-\frac{l}{2}, y\right), \quad f_1\left(\frac{l}{2}\right) = \frac{1}{d}\int_{-w/2-d}^{-w/2} dy f_B\left(\frac{l}{2}, y\right); \\
&f_2\left(-\frac{l}{2}\right) = \frac{1}{d}\int_{w/2}^{w/2+d} dy f_A\left(-\frac{l}{2}, y\right), \quad f_2\left(\frac{l}{2}\right) = \frac{1}{d}\int_{w/2}^{w/2+d} dy f_B\left(\frac{l}{2}, y\right); \\
&\frac{df_1}{dx}\left(-\frac{l}{2}\right) = \frac{1}{d}\int_{-w/2-d}^{-w/2} dy \left[\frac{\partial}{dx} f_A(x, y)\right]_{x=-l/2}, \quad \frac{df_1}{dx}\left(\frac{l}{2}\right) = \frac{1}{d}\int_{-w/2-d}^{-w/2} dy \left[\frac{\partial}{dx} f_A(x, y)\right]_{x=l/2}; \\
&\frac{df_2}{dx}\left(-\frac{l}{2}\right) = \frac{1}{d}\int_{w/2}^{w/2+d} dy \left[\frac{\partial}{dx} f_A(x, y)\right]_{x=-l/2}, \quad \frac{df_2}{dx}\left(\frac{l}{2}\right) = \frac{1}{d}\int_{w/2}^{w/2+d} dy \left[\frac{\partial}{dx} f_A(x, y)\right]_{x=l/2}.
\end{aligned} \tag{23}$$

From condition (16) follows the conservation laws for the x-components of the current densities

$$\begin{aligned} j_1\left(-\frac{l}{2},y,z\right) &= j_{Ax}\left(-\frac{l}{2},y,z\right), \\ j_1\left(\frac{l}{2},y,z\right) &= j_{Bx}\left(\frac{l}{2},y,z\right) \qquad \left(y\in\left(-\frac{w}{2}-d,-\frac{w}{2}\right), \quad z\in\left(-\frac{t}{2},\frac{t}{2}\right)\right); \\ j_2\left(-\frac{l}{2},y,z\right) &= j_{Ax}\left(-\frac{l}{2},y,z\right), \\ j_2\left(\frac{l}{2},y,z\right) &= j_{Bx}\left(\frac{l}{2},y,z\right) \qquad \left(y\in\left(\frac{w}{2},\frac{w}{2}+d\right), \quad z\in\left(-\frac{t}{2},\frac{t}{2}\right)\right) \end{aligned} \tag{24}$$

and

$$\frac{\partial j_1}{\partial x}=0, \quad \frac{\partial j_2}{\partial x}=0\left(x\in\left(-\frac{l}{2},\frac{l}{2}\right)\right), \tag{25}$$

as well as the conservation law for the total current I, which can be written in two equivalent forms:

$$\bar{j}_1+\bar{j}_2=J \tag{26}$$

and

$$\begin{aligned} &\bar{j}_1=J/2+\bar{j}_{\rm circ}, \ \bar{j}_2=J/2-\bar{j}_{\rm circ}, \\ &\bar{j}_{\rm circ}=\frac{1}{2}\left(\bar{j}_1-\bar{j}_2\right). \end{aligned} \tag{27}$$

Here, $J\equiv I/s$, $s=td$ is the cross-sectional area of each channel, and the average current densities in the channels are defined by the relations

$$\begin{aligned} \bar{j}_1 &\equiv \frac{1}{s}\int\limits_{-t/2}^{t/2}dz\int\limits_{-w/2-d}^{-w/2}dy\, j_1(y,z), \\ \bar{j}_2 &\equiv \frac{1}{s}\int\limits_{-t/2}^{t/2}dz\int\limits_{w/2}^{w/2+d}dy\, j_2(y,z). \end{aligned} \tag{28}$$

In the notation of Eq. (27), the quantity $\bar{j}_{circ}$ denotes the average density of the *circulating* current.

For a clear understanding of the oscillation effect of the *first order* in the parameter ξ/l, it is very important to keep in mind that, because of the conditions (6), the current densities j_1 and j_2 are non-uniform within the cross sections and cannot be taken from under the integral sing in the right-hand sides of Eq. (28). (The uniformity of the distributions of j_1 and j_2 requires strong inequalities $t, d\ll\lambda$.[4–6])

It is also important to keep in mind that the full current I can be expressed in terms of the current densities $j_{Ax,Bx}$ on the side surfaces of the electrodes:

$$\begin{aligned} I &= \lambda_\perp\int\limits_{-t/2}^{t/2}dz\left[j_{Ax}\left(-\infty,\frac{L_y}{2},z\right)+j_{Ax}\left(-\infty,-\frac{L_y}{2},z\right)\right] \\ &= \lambda_\perp\int\limits_{-t/2}^{t/2}dz\left[j_{Bx}\left(\infty,\frac{L_y}{2},z\right)+j_{Bx}\left(\infty,-\frac{L_y}{2},z\right)\right]. \end{aligned} \tag{29}$$

Relations (29), which are valid due to condition (9), are, in fact, the rigorous definitions of the penetration depth. As immediately follows from these relations, conservation law (26), and the inequality $d<\lambda_\perp$ in the left-hand side of Eq. (10), the average current densities $j_{Ax,Bx}$ on the side surfaces of the electrodes (the right-hand side of Eq. (29) with a factor of $1/(2\lambda_\perp t)$) is strictly less than the average current density in one of the channels ($\bar{j}_1$ and $\bar{j}_2$). For this reason, the experimentally observed value of the total critical current $I=I_c$ is determined specifically by the state of the narrow channels and not the wide electrodes.

To obtain another equation relating $\bar{j}_1$ and $\bar{j}_2$, we should use condition (13). Let the topological number N be given. Then we consider a set of equivalent contours Γ, which are rectangles in the cross-section plane $z=$ const. In each of the planes, let us denote the coordinates of the vertices of the rectangles as $(-x_0, y_1)$, (x_0, y_1), (x_0, y_2) and $(-x_0, y_2)$: see Fig. 1. The value x_0, satisfying the condition $x_0-l/2\gg\lambda_\perp$, is assumed to be given, while y_1 and y_2 can be varied independently within the width of the channels. Using definition (18), we express the phase gradient $\nabla\chi$ through the current densities $j_{1,2}$, $j_{Ax,Bx}$, and the vector potential $\mathbf{A}$. Given the conservation laws (25) and the condition $\mathbf{h}=0$, $\mathbf{j}=0$ on the sides of the rectangles parallel to the plane $x=0$, we obtain from Eq. (13) for each of the contours Γ lying in a given plane $z=z_0$:

$$\begin{aligned} &C_1 j_1(y_1,z_0)\left[1+\varepsilon_1(y_1,z_0)\right]-C_2 j_2(y_2,z_0)\left[1+\varepsilon_2(y_2,z_0)\right] \\ &\quad = 3\sqrt{3}\pi j_{c0}\frac{\xi}{l}\left(N-\frac{\Phi_{y_1,y_2,z_0}}{\Phi_0}\right), \end{aligned} \tag{30}$$

where

$$C_1\equiv C_1[f_1]=\frac{1}{l}\int\limits_{-l/2}^{l/2}\frac{dx}{f_1^2(x)}, \quad C_2\equiv C_2[f_2]=\frac{1}{l}\int\limits_{-l/2}^{l/2}\frac{dx}{f_2^2(-x)}; \tag{31}$$

$$\begin{aligned} \varepsilon_1(y_1,z_0) &= \frac{\displaystyle\int\limits_{-x_0}^{-l/2}\frac{dx\, j_{Ax}(x,y_1,z_0)}{f_A^2(x,y_1)}+\int\limits_{l/2}^{x_0}\frac{dx\, j_{Bx}(x,y_1,z_0)}{f_B^2(x,y_1)}}{lC_1 j_1(y_1,z_0)}>0, \\ \varepsilon_2(y_2,z_0) &= \frac{\displaystyle\int\limits_{-x_0}^{-l/2}\frac{dx\, j_{Ax}(-x,y_2,z_0)}{f_A^2(-x,y_2)}+\int\limits_{l/2}^{x_0}\frac{dx\, j_{Bx}(-x,y_2,z_0)}{f_B^2(-x,y_2)}}{lC_2 j_2(y_2,z_0)}>0; \end{aligned} \tag{32}$$

$$j_{c0} = \frac{c\Phi_0}{12\sqrt{3}\pi^2\lambda^2\xi} \tag{33}$$

is the critical superconducting current density in the Ginzburg-Landau approximation,[4–6] and Φ_{y_1,y_2,z_0} is the flux of the magnetic field **h** through the contour under consideration:

$$\Phi_{y_1,y_2,z_0} = \int_{y_1}^{y_2} dy \int_{-l/2}^{l/2} dx\, h_z(x,y,z_0) + \lambda_\perp \int_{y_1}^{y_2} dy \left[h_z\left(\frac{l}{2},y,z_0\right) + h_z\left(-\frac{l}{2},y,z_0\right)\right]. \tag{34}$$

Using the continuity conditions (24), obvious inequality $0 < f_{1,2} \le f_{A,B} \le 1$, and the definition of the penetration depth $\lambda_\perp$ (see Eq. (29)), we can easily obtain a rigorous upper bound for the values of Eq. (32):

$$0 < \varepsilon_1(y_1,z_0), \quad \varepsilon_2(y_2,z_0) \le \frac{2\lambda_\perp}{l} < \frac{2\xi}{l} \ll 1. \tag{35}$$

Therefore, the terms $\varepsilon_{1,2}$ may be omitted in Eq. (30) containing a small parameter ξ/l in the right-hand side. This equation is obviously true for arbitrary values of the topological number N. Therefore, after averaging, we obtain:

$$C_1\bar{j}_1 - C_2\bar{j}_2 = 3\sqrt{3}\pi j_{c0}\frac{\xi}{l}\left(N - \frac{\bar{\Phi}}{\Phi_0}\right)(N = 0, \pm1, \pm2, ...), \tag{36}$$

$$\bar{\Phi} \equiv \frac{1}{sd}\int_{-t/2}^{t/2} dz_0 \int_{w/2}^{w/2+d} dy_2 \int_{-w/2-d}^{-w/2} dy_1 \Phi_{y_1,y_2,z_0} \tag{37}$$

is the flux of the magnetic field **h** through the opening in the system, averaged over all equivalent contours Γ.

Due to the symmetry of the system, in the state of thermodynamic equilibrium $\bar{\Phi} = \bar{\Phi}(H_e)$, and $\bar{\Phi}(0) = 0$. In a general case, the average flux $\bar{\Phi}$ may be represented as follows:

$$\bar{\Phi} = \bar{\Phi}_e + \frac{s}{c}\mathcal{L}\bar{j}_{\text{circ}}, \tag{38}$$

where

$$\bar{\Phi}_e = (2\lambda_\perp + l)(w + d)H_e \tag{39}$$

is the average flux of the magnetic field $\mathbf{H}_e$ and $\mathcal{L}$ is the geometrical inductance of system[25] which is considered as known.

To obtain a closed system of equations we should also specify an algorithm for computing the reduced order parameters $f_{1,2}$ in definition (31). Let's start with a rigorous formulation of the problem, which includes the one-dimensional Ginzburg-Landau equations

$$\xi^2\frac{d^2 f_{1,2}}{dx^2} + \left[1 - f_{1,2}^2 - \frac{4\overline{j_{1,2}^2}}{27 j_{c0}^2}\frac{1}{f_{1,2}^4}\right] f_{1,2} = 0 \tag{40}$$

(see, e.g., Ref. 16) and continuity conditions (23) at the boundaries of the electrodes. (As usual, the bar over the quantities $j_{1,2}^2$ in Eq. (40) denotes averaging over the coordinates y and z.) Now, we will show that in our case the problem (23), (40) allows a substantial simplification.

Indeed, the effect of boundaries extends only to a distance of about ξ, which is small (due to condition (8)) compared with the length of the channel l. On the other hand, for our purposes it is sufficient to consider the main region $-l/2 + \xi < x < l/2 - \xi$, where one can neglect the second derivatives in Eq. (40) and ignore the boundary conditions (23). (This approximation introduces an error of about ξ^2/l^2, which is absolutely insignificant when the oscillation effect of the first order in the parameter ξ/l is considered.)

If, additionally, the approximation $\overline{j_{1,2}^2} \approx \bar{j}_{1,2}^2$ is taken, which is rather natural given conditions (6) and (7), we arrive at non-linear algebraic equations:

$$f_{1,2}^4\left(1 - f_{1,2}^2\right) = \frac{4\bar{j}_{1,2}^2}{27 j_{c0}^2}. \tag{41}$$

Equations (26), (27), (36), (38), and (41) do not contain unknown physical quantities related to the electrodes and allow for a straightforward solution.

From Eqs. (27), (36), and (38) we find:

$$\bar{j}_1 = \frac{J}{2} + \bar{j}_{\text{circ}}, \quad \bar{j}_2 = \frac{J}{2} - \bar{j}_{\text{circ}},$$
$$\bar{j}_{\text{circ}} = \frac{1}{C_1 + C_2 + 2\Lambda}\left[\frac{(C_2 - C_1)J}{2} + \frac{3\sqrt{3}\pi\xi j_{c0}}{l}\left(N - \frac{\bar{\Phi}_e}{\Phi_0}\right)\right] \quad (N = 0, \pm1, \pm2, ...), \tag{42}$$

where

$$\Lambda \equiv \frac{1}{8\pi}\frac{s}{\lambda^2}\frac{\mathcal{L}}{l}, \tag{43}$$

$$C_1 \equiv 1/f_1^2, \quad C_2 \equiv 1/f_2^2, \tag{44}$$

and the constants $f_{1,2}^2$ satisfy Eq. (41). To begin with, let us discuss the solution of Eqs. (41)–(44) in two simple limiting cases.

Let $H_e = 0$ and $J \ge 0$. At the thermodynamic equilibrium, $N = 0$. Due to the symmetry, $C_1 = C_2$, and

$$\bar{j}_1 = \bar{j}_2 = J/2. \tag{45}$$

The square of the order parameter $f_{J/2}^2 \equiv f_1^2 = f_2^2$ is given by the solution of Eq. (41), where we should assume $j_1 = j_2 = \text{J}/2$.

The total critical current of the system is determined by a simple expression:

$$I_c \equiv sJ_c = 2s\bar{j}_c, \tag{46}$$

where $\bar{j}_c$ is the critical value of mean current density in each of the channels. Non-uniform densities $j_{1,2}$ have the maximum values on the surface of the channels. The critical value of $\bar{j}_c$ is achieved when the surface densities $j_{1,2}$ become equal to the critical density j_{c0} as defined by Eq. (33). Therefore, we find:

$$\bar{j}_c \le j_{c0}. \tag{47}$$

Note that in the case of complete uniformity of the distribution of current densities $j_{1,2}$, relation (47) is reduced to a strict equality. In contrast, in experiments on narrow

channels the strict inequality $\bar{j}_c < j_{c0}$ is always realized.[5] In our case we have a two-sided inequality:

$$\frac{\xi}{l} j_{c0} \ll \bar{j}_c < j_{c0}. \tag{48}$$

Now let $J = 0$, and $H_e \geq 0$. Like in the previous case, $C_1 = C_2$, and the average density of the circulating current induced by an external field H_e is given by

$$\bar{j}_{\text{circ}} \equiv \bar{j}_1 = -\bar{j}_2 = \frac{3\sqrt{3}\pi f^2_{\bar{j}_{\text{circ}}}}{2\left(1 + f^2_{\bar{j}_{\text{circ}}}\Lambda\right)} \frac{\xi}{l} j_{c0} \left(N - \frac{\bar{\Phi}_e}{\Phi_0}\right),$$
$$(N = 0, \pm 1, \pm 2, \ldots) \tag{49}$$

where the square of the order parameter $f^2_{\bar{j}_{circ}} \equiv f_1^2 = f_2^2$ satisfies Eq. (41) provided $\bar{j}_1 = -\bar{j}_2 = \bar{j}_{circ}$.

It is well-known[8,26] that the role of the topological number N is to minimize the electromagnetic energy of circulating currents. For this reason, stable (equilibrium) states and low-lying metastable (nonequilibrium) states should satisfy the condition

$$\max_N \left| N - \frac{\bar{\Phi}_e}{\Phi_0} \right| \sim 1. \tag{50}$$

Such states allow to use the perturbation theory in the small parameter ξ/l. In the first approximation, which is of interest here, we have: $f^2_{\bar{j}_{circ}} = 1 + o(\xi/l)$ and

$$\bar{j}_{\text{circ}} = \frac{3\sqrt{3}\pi}{2(1+\Lambda)} \frac{\xi}{l} j_{c0} \left(N - \frac{\bar{\Phi}_e}{\Phi_0}\right) + o\left(\frac{\xi}{l}\right)$$
$$\left(\max_N \left| N - \frac{\bar{\Phi}_e}{\Phi_0} \right| \sim 1\right), \tag{51}$$

where $o(\xi/l)$ denotes the contribution of terms of the order $(\xi/l)^n$ with the exponents $n > 1$.

It is important to note that for equilibrium and weakly nonequilibrium states the maximum value of $\bar{j}_{circ}$ is much smaller than the critical value of the average density j_c due to the condition (48). However, this conclusion could break down in the case of strongly nonequilibrium states when condition (50) is not satisfied and the perturbation theory in the parameter ξ/l becomes inapplicable.

In the opposite limiting case of pure equilibrium states, expression (51) takes the following form:

$$\bar{j}_{\text{circ}} = -\frac{3\sqrt{3}\pi}{2(1+\Lambda)} \frac{\xi}{l} j_{c0} \Theta\left(\frac{\bar{\Phi}_e}{\Phi_0}\right) + o\left(\frac{\xi}{l}\right), \tag{52}$$

where the periodic piecewise linear function $\Theta = \Theta(x)$ is given by[26]

$$\Theta(x) = \begin{cases} \{x\} & \{x\} \leq 1/2; \\ -1 + \{x\}, & \{x\} > 1/2, \end{cases} \tag{53}$$

where $\{x\}$ denotes the fractional part of x. From Eqs. (52) and (53) follows that, for instance, the transitions between different equilibrium states $N \leftrightarrow N + 1$ occur upon satisfying the condition $\bar{\Phi}_e/\Phi_0 = (2N + 1)/2$. At the transition points $N \leftrightarrow N + 1$, the circulating current $\bar{j}_{circ}$ changes sign. The sign change of $\bar{j}_{circ}$ also occurs at the points $\bar{\Phi}_e/\Phi_0 = N$, see the graph of the dependence $\tilde{\bar{j}}_{circ} = \tilde{\bar{j}}_{circ}(\bar{\Phi}_e/\Phi_0)$ in Fig. 9, where

$$\tilde{\bar{j}}_{\text{circ}} \equiv \frac{\bar{j}_{\text{circ}}}{\frac{3\sqrt{3}\pi}{2(1+\Lambda)} \frac{\xi}{l} j_{c0}}$$

is the reduced average density of the circulating current. We also note that the absolute value of the average magnetic flux induced by circulating current does not exceed $\Phi_0/2$ in the equilibrium case:

$$\frac{s}{c} \mathcal{L} |\bar{j}_{\text{circ}}| = \frac{|\Theta(\bar{\Phi}_e/\Phi_0)| \Lambda \Phi_0}{(1+\Lambda)} \leq \frac{1}{2} \frac{\Lambda \Phi_0}{(1+\Lambda)} < \frac{\Phi_0}{2}. \tag{54}$$

Let us finally consider the general case, when $J \geq 0$ and $H_e \geq 0$. It is *a priory* clear that the average current densities $j_{1,2}$ cannot be equal to a simple sum of the contributions (45) and (49) because now the $C_1 \neq C_2$. Nevertheless, the linear parts of the dependences of interest $\bar{j}_{1,2} = \bar{j}_{1,2}(\bar{\Phi}/\Phi_0)$ can be easily found using the perturbation theory. (Of course, it is assumed in this case that the condition (50) is satisfied.)

In the first approximation in the small parameter ξ/l, the solutions of equations (41) are as follows:

$$f_1^2 = f_{J/2}^2 - \frac{2\sqrt{3}\pi}{9 f_{J/2}^2 \left(1 + f_{J/2}^2 \Lambda\right) j_{c0}} \frac{J\xi}{l} \left(N - \frac{\bar{\Phi}_e}{\Phi_0}\right) + o\left(\frac{\xi}{l}\right),$$
$$f_1^2 = f_{J/2}^2 + \frac{2\sqrt{3}\pi}{9 f_{J/2}^2 \left(1 + f_{J/2}^2 \Lambda\right) j_{c0}} \frac{J\xi}{l} \left(N - \frac{\bar{\Phi}_e}{\Phi_0}\right) + o\left(\frac{\xi}{l}\right)$$
$$\left(\max_N \left| N - \frac{\bar{\Phi}_e}{\Phi_0} \right| \sim 1\right), \tag{55}$$

where the square of the unperturbed order parameter $f^2_{J/2}$ satisfies the equation

$$f^4_{J/2}\left(1 - f^2_{J/2}\right) = \frac{J^2}{27 j_{c0}^2}. \tag{56}$$

Substituting Eq. (55) into Eqs. (42) and (44) leads to the desired linear dependences:

$$\bar{j}_1 = \frac{1}{2}\left[J + 3\sqrt{3}\pi \frac{\xi}{l} j_{c0} \frac{f^2_{J/2}}{1 + f^2_{J/2}\Lambda} \left(1 - \frac{2}{27 f^6_{J/2}\left(1 + f^2_{J/2}\Lambda\right)} \frac{J^2}{j_{c0}^2}\right)\left(N - \frac{\bar{\Phi}_e}{\Phi_0}\right)\right] + o\left(\frac{\xi}{l}\right),$$
$$\bar{j}_2 = \frac{1}{2}\left[J - 3\sqrt{3}\pi \frac{\xi}{l} j_{c0} \frac{f^2_{J/2}}{1 + f^2_{J/2}\Lambda} \left(1 - \frac{2}{27 f^6_{J/2}\left(1 + f^2_{J/2}\Lambda\right)} \frac{J^2}{j_{c0}^2}\right)\left(N - \frac{\bar{\Phi}_e}{\Phi_0}\right)\right] + o\left(\frac{\xi}{l}\right), \tag{57}$$
$$\max_N \left| N - \frac{\bar{\Phi}_e}{\Phi_0} \right| \sim 1.$$

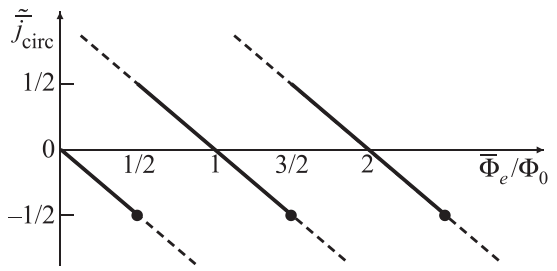

FIG. 9. Dependence $\tilde{\bar{j}}_{circ} = \tilde{\bar{j}}_{circ}(\bar{\Phi}_e/\Phi_0)$. Solid and dashed lines correspond to the equilibrium and metastable states, respectively.

As we see, in the presence of the transport current, the amplitude of the circulating current is suppressed (cf. the second terms in Eqs. (57) and (51)).

As could be expected, in the corresponding limiting cases, Eq. (57) is reduced to Eqs. (45) and (51).

In the general case the average current densities j_1 and j_2 are not equal to each other. Therefore, the critical value of the total current $I = I_c \equiv sJ_c$ is reached under an obvious condition

$$\max\{\bar{j}_1, \bar{j}_2\} = \bar{j}_c. \tag{58}$$

From condition (58) and equations (57) we can easily obtain:

$$J_c \equiv \frac{I_c}{s} = 2\bar{j}_c - 3\sqrt{3}\pi\frac{\xi}{l}j_{c0}\frac{f^2_{\bar{j}_c}}{1+f^2_{\bar{j}_c}\Lambda} \times \left[1 - \frac{8}{27 f^6_{\bar{j}_c}\left(1+f^2_{\bar{j}_c}\Lambda\right)}\frac{\bar{j}_c^2}{j_{c0}^2}\right]\left|N - \frac{\bar{\Phi}_e}{\Phi_0}\right| + o\left(\frac{\xi}{l}\right),$$
$$\max_N\left|N - \frac{\bar{\Phi}_e}{\Phi_0}\right| \sim 1. \tag{59}$$

In the case of pure equilibrium states, the expression (59) reduces to

$$J_c \equiv \frac{I_c}{s} = 2\bar{j}_c - 3\sqrt{3}\pi\frac{\xi}{l}j_{c0}\frac{f^2_{\bar{j}_c}}{1+f^2_{\bar{j}_c}\Lambda} \times \left[1 - \frac{8}{27 f^6_{\bar{j}_c}\left(1+f^2_{\bar{j}_c}\Lambda\right)}\frac{\bar{j}_c^2}{j_{c0}^2}\right]\left|\Theta\left(\frac{\bar{\Phi}}{\Phi_0}\right)\right| + o\left(\frac{\xi}{l}\right), \tag{60}$$

where the function $\Theta = \Theta(x)$ is given by definition (53). As follows from Eqs. (47) and (56), the value of $f^2_{\bar{j}_c}$ appearing in the right-hand sides of Eqs. (59) and (60) satisfies the two-sided inequality:

$$\frac{2}{3} \le f^2_{j_c} < 1. \tag{61}$$

As can be seen from the graph of $\Delta\tilde{J}_c = \Delta\tilde{J}_c(\bar{\Phi}_e/\Phi_0)$ shown in Fig. 10, where

$$\Delta\tilde{J}_c \equiv \frac{J_c - 2\bar{j}_c}{3\sqrt{3}\pi\frac{\xi}{l}j_{c0}\frac{f^2_{\bar{j}_c}}{1+f^2_{\bar{j}_c}\Lambda}\left[1 - \frac{8}{27 f^6_{\bar{j}_c}\left(1+f^2_{\bar{j}_c}\Lambda\right)}\frac{\bar{j}_c^2}{j_{c0}^2}\right]}$$

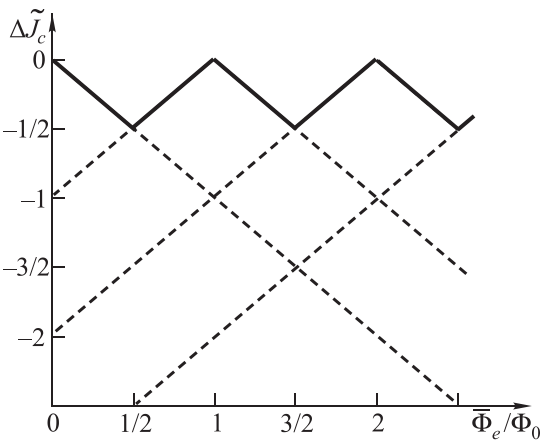

FIG. 10. Dependence $\Delta\tilde{J}_c = \Delta\tilde{J}_c(\bar{\Phi}_e/\Phi_0)$. As in Fig. 9, solid and dashed lines correspond to the equilibrium and metastable states, respectively.

is the reduced amplitude of the critical current oscillations, Eqs. (59) and (60) together give an adequate theoretical description of the oscillation effect of the first order, which was observed in our experiment. As follows from condition (58) and Eq. (57), the critical value of the average current density $\bar{j}_c$ is achieved alternately in each of the contacts which is also confirmed experimentally. Thus, for positive values of the circulating current the condition $\bar{j}_1 = \bar{j}_c$, $\bar{j}_2 < \bar{j}_c$ is satisfied, while for negative values the condition $\bar{j}_2 = \bar{j}_c, \bar{j}_1 < \bar{j}_c$ is satisfied.

As can be easily concluded from Eqs. (59) and (60), conditions (6) are optimal for observation of this effect. We illustrate this conclusion with two important examples.

Let us first consider the case of very narrow and thin channels when the strong inequalities $t, d \ll \lambda$ are satisfied, hence ensuring the uniformity of the distribution of the current densities $j_{1,2}$ and the equality $\bar{j}_c = j_{c0}$. Obviously, in this case, expressions (59) and (60) remain valid, and $f^2_{\bar{j}_c} = f^2_{\bar{j}_{c0}} = 2/3$. If, additionally, $\Lambda \ll 1$ (negligible screening of the external field), Eq. (60) takes the following form:

$$J_c = 2j_{c0} - \frac{4\pi}{\sqrt{3}}\frac{\xi}{l}j_{c0}\Lambda\left|\Theta\left(\frac{\bar{\Phi}_e}{\Phi_0}\right)\right| + o\left(\frac{\xi}{l}\right). \tag{62}$$

As we can see, the relative amplitude of the oscillation effect is significantly reduced due to the appearance of the factor $\Lambda \ll 1$.

Expressions (59) and (60) remain valid also when, in place of conditions (5) and (6), the following conditions are satisfied

$$d \sim \lambda, \quad t \gg \xi. \tag{63}$$

If additionally the condition of strong screening of the external field $\Lambda \gg 1$ is also satisfied, then from Eq. (60) we obtain:

$$J_c = 2\bar{j}_c - 3\sqrt{3}\pi\frac{\xi}{l}\frac{j_{c0}}{\Lambda}\left|\Theta\left(\frac{\bar{\Phi}_e}{\Phi_0}\right)\right| + o\left(\frac{\xi}{l}\right), \tag{64}$$

which implies the suppression of the relative amplitude of the oscillation effect due to the factor $\Lambda^{-1} \ll 1$. It is interesting to note that expression (64) can be represented in the

form coinciding with that in Ref. 18, in which it has been obtained for the case of a superconducting interferometer containing two identical point contacts:

$$J_c = 2\bar{j}_c - \frac{2c\Phi_0}{s\mathcal{L}}\left|\Theta\left(\frac{\bar{\Phi}_e}{\Phi_0}\right)\right| + o\left(\frac{\xi}{l}\right). \qquad (65)$$

4. Conclusion

The results of experimental and theoretical investigations of a new macroscopic oscillation effect in macroscopic doubly-connected superconducting structures not containing Josephson junctions were presented.

It was shown experimentally (Sec. 2) that the critical current I_c of a thin-film tin structure, which is shown in Fig. 1 and satisfies the macroscopicity condition $l \gg \xi$, exhibits the periodic (with a period equal to Φ_0) dependence on the average external magnetic flux $\bar{\Phi}_e$ at temperatures close to T_c. All the dependences $I_c = I_c(\bar{\Phi}_e)$ obtained in our experiments showed a pronounced piecewise linear behavior and were multivalued (there were branches corresponding to metastable states). Furthermore, the oscillation amplitude of I_c at a given temperature was found to be inversely proportional to the length of the superconducting channel l.

The above features of the macroscopic oscillation effect were rigorously explained within the theory presented in Sec. 3. This theory is based on the local Ginzburg-Landau approximation and relates to a perfectly symmetric system. At the end of Sec. 3, we demonstrated that the material and the sample parameters used in our experiments correspond to the optimum conditions required for the observation of the effect.

We also observed experimentally the shifts of maxima in the dependences $I_c = I_c(\bar{\Phi}_e)$ accompanied by an asymmetry with respect to the change of the transport current direction, which were related to an incomplete symmetry of the samples employed. Qualitatively, these effects can be explained by the inequality of the critical currents of the superconducting channels (see the end of Sec. 2). However, their rigorous theoretical description is beyond the scope of this paper and requires separate consideration.

The authors thank J. Koval (University of Erlangen, Germany) for the fabrication of high-quality samples by electron beam lithography and A. V. Ustinov (Institute of Technology, Karlsruhe, Germany) for a stimulating discussion of the experimental results.

[a]Email: sivakov@ilt.kharkov.ua

[1]C. N. Yang, Rev. Mod. Phys. **34**, 694 (1962).
[2]N. N. Bogolyubov, *Quasi-averages in Problems of Statistical Physics, Preprint R-1451* (Joint Institute of Nuclear Research, Dubna, 1963) [in Russian].
[3]W. A. Little and R. D. Parks, Phys. Rev. Lett. **9**, 9 (1962); R. D. Parks and W. A. Little, Phys. Rev. **133**, A97 (1964).
[4]P. G. de Gennes, *Superconductivity of Metals and Alloys* (Benjamin, New York, 1966).
[5]M. Tinkham, *Introduction to Superconductivity* (McGraw-Hill, New York, 1996).
[6]A. A. Abrikosov, *Fundamentals of the Theory of Metals* (North-Holland, Amsterdam, 1988).
[7]X. Zhang and J. C. Price, Phys. Rev. B **55**, 3128 (1997).
[8]Y. S. Yerin, S. V. Kuplevakhsky, and A. N. Omelyanchouk, Fiz. Nizk. Temp. **34**, 1131 (2008) [Low Temp. Phys. **34**, 891 (2008)].
[9]J. E. Zimmerman and A. H. Silver, Phys. Rev. **141**, 367 (1966).
[10]L. Solymar, *Superconductive Tunnelling and Applications* (Chapman and Hall, London, 1972).
[11]A. Barone and G. Paterno, *Physics and Applications of the Josephson Effect* (Wiley, New York, 1982).
[12]A. G. Sivakov, Y. Koval, A. M. Glukhov, A. N. Omelyanchouk, P. Müller, and A. V. Ustinov, Phys. Rev. Lett. **91**, 267001 (2003).
[13]V. V. Moshchalkov, L. Gielen, M. Dhalle, C. Van Haesendonck, and Y. Bruynseraede, Nature (London) **361**, 617 (1993).
[14]V. L. Gurtovoĭ, S. V. Dubonos, S. V. Karpiĭ, A. V. Nikulov, and V. A. Tulin, Zh. Éksp. Teor. Fiz. **132**, 297 (2007) [JETP **105**, 262 (2007)]; V. L. Gurtovoĭ, S. V. Dubonos, A. V. Nikulov, N. N. Osipov, and V. A. Tulin, Zh. Éksp. Teor. Fiz. **132**, 1320 (2007) [JETP **105**, 1157 (2007)].
[15]S. Michotte, D. Lucot, and D. Mailly, Phys. Rev. B **81**, 100503R (2010).
[16]J. Fink, V. Grunfeld, and A. Lopez, Phys. Rev. B **35**, 35 (1987); H. J. Fink, J. Loo, and S. M. Roberts, *ibid.* **37**, 5050 (1988).
[17]V. L. Ginzburg and L. D. Landau, Zh. Éksp. Teor. Fiz. **20**, 1064 (1950) [English translation in *Men of Physics: L. D. Landau*, edited by D. ter Haar (Pergamon, New York, 1965), Vol. 1, pp. 138–167].
[18]A. Th. A. M. De Waele and R. De Bruyn Ouboter, Physica **41**, 225 (1969).
[19]T. A. Fulton, L. Dunkleberger, and B. C. Dynes, Phys. Rev. B **6**, 855 (1972).
[20]J. Bardeen, L. N. Cooper, and J. R. Schrieffer, Phys. Rev. **108**, 1175 (1957).
[21]B. I. Ivlev and N. B. Kopnin, Usp. Fiz. Nauk **142**, 435 (1984) [Sov. Phys. Usp. **27**, 206 (1984)].
[22]J. Pearl, Appl. Phys. Lett. **5**, 65 (1964).
[23]See the discussion of the conditions of uniqueness in E. Mertzbacher, Am. J. Phys. **30**, 237 (1962).
[24]R. Rajaraman, *Solitons and Instantons in Quantum Field Theory* (North-Holland, Amsterdam, 1982).
[25]I. E. Tamm, *Fundamentals of the Theory of Electricity* (Nauka, Moscow, 1976) [in Russian].
[26]S. V. Kuplevakhsky, A. N. Omelyanchouk, and Y. S. Yerin, Fiz. Nizk. Temp. **37**, 842 (2011) [Low Temp. Phys. **37**, 667 (2011)].

Translated by L. Gardt